Research Article

Percutaneous Penetration Modifiers and Formulation Effects: Thermal and Spectral Analyses

Diksha Kaushik[1] and Bozena Michniak-Kohn[1,2,3]

Abstract. The study investigated the formulation effects of laurocapram and iminosulfurane derived penetration modifiers on human stratum corneum using thermal and spectral analyses. Firstly, formulations of penetration modifiers were assessed as enhancers/retardants using the model permeant, diethyl-*m*-toluamide followed by investigation of their mechanisms of action using differential scanning calorimetry (DSC) and attenuated total reflectance Fourier-transform infra-red spectroscopy. The penetration modifiers investigated were laurocapram, 3-dodecanoyloxazolidin-2-one (N-0915), *S,S*-dimethyl-*N*-(4-bromobenzoyl) iminosulfurane (DMBIS), *S,S*-dimethyl-*N*-(2-methoxycarbonylbenzene-sulfonyl) iminosulfurane (DMMCBI) and *tert*-butyl 1-dodecyl-2-oxoazepan-3-yl-carbamate (TBDOC) that were formulated in either water, propylene glycol (PG), ethanol or polyethylene glycol 400 (PEG 400). The results explain the mechanism for the first time why an enhancer can become a retardant or *vice versa* depending upon the vehicle in which it is applied to the skin. DSC indicated that penetration modifier formulations enhanced permeation of active mainly by disruption and fluidization of the stratum corneum lipid bilayers while IR data indicated characteristic blue shifts with decreases in peak intensity. On the other hand, DSC of penetration modifier formulations showing retardation depicted elevated T_{m2} with a strengthening of lipid–protein complex while IR results indicated formation of multiple peaks around 1,738 cm^{-1} transition in stratum corneum spectra suggesting retardation may be caused by organization of SC lipids by increased H-bonding.

KEY WORDS: differential scanning calorimetry; enhancers; infra-red spectroscopy; penetration modifiers; retardants; stratum corneum.

INTRODUCTION

Stratum corneum (SC) is a complex tissue that provides a barrier to most permeants due to its unique composition and organization of lipids and proteins present within it (1). In order to modify the barrier properties of the SC, enhancers and retardants have been developed where enhancers act by disrupting the lipid bilayer within the SC and retardants act by strengthening the lipid organization of the SC (2). Up to now, known enhancer molecules were always thought to

cause enhancement of the permeant, and retardants were expected to decrease the permeation of the active irrespective of the formulation components.

However, we recently discovered that an enhancer can become a retardant, or *vice versa*, for a specific permeant (diethyl-*m*-toluamide, DEET) depending upon the vehicle in which it is applied to the skin (3). In a previous study, we investigated the effect of five percutaneous penetration modifiers (laurocapram, 3-dodecanoyloxazolidin-2-one (*N*-0915), *S,S*-dimethyl-*N*-(4-bromobenzoyl) iminosulfurane (DMBIS), *S,S*-dimethyl-*N*-(2-methoxycarbonylbenzenesul-fonyl) iminosulfurane (DMMCBI) and *tert*-butyl 1-dodecyl-2-oxoazepan-3-yl-carbamate (TBDOC)) on permeation of model permeant DEET. The formulations of the above penetration modifiers were formulated in either water, propylene glycol (PG), ethanol or polyethylene glycol 400 (PEG 400). The penetration modifiers selected were either nitrogen-containing (laurocapram, N-0915, TBDOC) or sulfur-containing (DMBIS, DMMCBI) compounds. Another criterion for selection of penetration modifiers was that some of the selected penetration modifiers such as laurocapram, DMBIS have been known to act as enhancers (4,5) while rest of the modifiers in the study namely N-0915, DMMCBI and TBDOC are known to have retardant activity (6–8). Solvents used in the formulations were water, ethanol, PG, and PEG 400 that are not only commonly used vehicles in dermal

[1] Ernest Mario School of Pharmacy, Rutgers—The State University of New Jersey, Piscataway, New Jersey 08854, USA.

[2] New Jersey Center for Biomaterials, Rutgers—The State University of New Jersey, Piscataway, New Jersey 08854, USA.

[3] To whom correspondence should be addressed. (e-mail: michniak@biology.rutgers.edu)

ABBREVIATIONS: ATR-FTIR, Attenuated total reflectance Fourier-transform infra-red spectroscopy; DEET, Diethyl-*m*-toluamide; DMBIS, *S,S*-Dimethyl-*N*-(4-bromobenzoyl) iminosulfurane; DMMCBI, *S,S*-dimethyl-*N*-(2-methoxycarbonylbenzenesulfonyl) iminosulfurane; DSC, Differential scanning calorimetry; H, Mean enthalpy; H-bond, Hydrogen bond; HSD, Honestly significantly different; N-0915, 3-Dodecanoyloxazolidin-2-one; PEG 400, Polyethylene glycol 400; PG, Propylene glycol; SC, Stratum corneum; TBDOC, *tert*-Butyl 1-dodecyl-2-oxoazepan-3-yl-carbamate; T_m, Mean transition temperature.

formulations, but some are also good penetration modifiers (9). DEET was chosen as the permeant in the previous study since it is a liquid under ambient conditions and in this way we avoided the added complication of other vehicles and solubility issues. Moreover, DEET has been used as a model permeant in evaluation of numerous skin permeation/retardation studies (10,11). Results from permeation studies indicated that laurocapram enhanced DEET permeation in PG, but retarded in PEG 400. Similarly, N-0915 was a retardant of DEET with ethanol and PEG 400, but not with water. DMBIS decreased the permeation with ethanol as compared to permeation with water, PEG 400, or PG. Likewise, DMMCBI showed retardation of DEET with ethanol and PEG 400, but not with water or PG. TBDOC formulations showed retardation with ethanol, but behaved as enhancer with water, PG, and PEG 400. The mean flux values have been summarized in Table I (3). Suitable controls were performed to determine whether the enhancement/retardation effect was due to permeant-vehicle effect or permeant-penetration modifier effect (3).

In order to understand the mechanism by which the properties of enhancers/retardants change in a given vehicle, molecular investigation of SC was performed using differential scanning calorimetry (DSC) and attenuated total reflection-Fourier-transform infra-red spectroscopy (ATR-FTIR). Therefore, the objective of this paper was to investigate molecular changes in stratum corneum after treatment with different formulations of laurocapram, N-0915, DMBIS, DMMCBI and

TBDOC using the two analytical methods of DSC and ATR-FTIR that provide independent yet complementary information regarding the interaction of enhancer/retardants within the SC (12,13). Though there are reports of DEET affecting SC when used as enhancer to increase the permeation of drugs (14), in our previous study (3), DEET was merely used as a model permeant to evaluate the permeation effects of penetration modifier formulations. However, in the current study, our main objective was to understand the mechanism of action of laurocapram and iminosulfurane derived penetration modifiers. Therefore, to achieve our objective, we planned experiments in such a way that involved no addition of DEET after application of penetration modifier formulations.

MATERIALS AND METHODS

Materials

Chemicals

3-Dodecanoyloxazolidin-2-one (N-0915), TBDOC were obtained as generous gifts from Dr. James Chapman at the University of South Carolina, Columbia, SC. Laurocapram, DMBIS, DMMCBI were provided by New Jersey Center for Biomaterials (Piscataway, NJ). Propylene glycol, ethanol, trypsin (Type 1) were purchased from Sigma Aldrich and polyethylene glycol 400 (PEG 400), phosphate buffer saline tablets were obtained from Fisher Chemicals. All other chemicals used were of analytical grade.

Skin Membranes

All human skin samples were purchased from New York Fire Fighters Skin Bank (New York) that were surgically removed within 24 h of the time of death of individuals and dermatomed to approximately 250–300 μm. All skin samples obtained were derived from left posterior leg of male and female individuals aged between 30 and 60 years. These skin pieces were stored at −80°C until use, but for no longer than 2 months.

Methods

Preparation of Formulations

The preparation of the penetration modifier formulation was as reported by Kaushik *et al.* (3). Briefly, weighed amount of penetration modifiers (laurocapram, N-0915, TBDOC, DMBIS, DMMCBI) were added to one of four vehicles (water, propylene glycol, ethanol, and PEG 400) to prepare 0.4 M solutions or suspensions. The solution/suspension was then vortexed at room temperature for 48 h. In case where suspension was obtained, centrifugation was performed at 8,000 rpm for 5 min to collect the supernatant and filtered supernatant was used as the final formulation for *in vitro* skin treatment. All formulations used in the study had 0.4 M concentrations of penetration modifiers or were saturated solution of penetration modifiers (with comparable thermodynamic activity). The available amounts of penetration modifiers in each vehicle were as reported by Kaushik *et al.* (3).

Table I. Mean Flux of DEET in Presence of Laurocapram and Iminosulfurane Analogues in Selected Vehicles (3)

Treatments	Mean flux, J (μg/cm^2 h)	MR$_J{}^a$
No treatment	58.0±19.4	1.0
Water	168.2±22.9^b	2.9
PG	256.0±61.7^b	4.4
Ethanol	112.6±23.2^b	1.9
PEG 400	25.6±12.2^b	0.4
Laurocapram	122.3±26.8^b	2.1
Laurocapram–water	268.3±37.4^b	4.6
Laurocapram–PG	291.2±18.1^b	5.1
Laurocapram–ethanol	111.5±7.9^b	1.9
laurocapram–PEG 400	18.4±4.9^b	0.3
N-0915–water	154.4±28.6^b	2.7
N-0915–PG	48.8±15.8	0.8
N-0915–ethanol	16.3±4.1^b	0.3
N-0915–PEG 400	14.7±4.7^b	0.2
DMBIS–water	178.0±7.1^b	1.8
DMBIS–PG	335.0±22.0^b	3.4
DMBIS–ethanol	150.1±14.9^b	1.5
DMBIS–PEG 400	192.8±8.2^b	1.9
DMMCBI–water	143.1±44.7^b	2.5
DMMCBI–PG	67.7±25.9	1.2
DMMCBI–ethanol	37.3±0.2	0.6
DMMCBI–PEG 400	36.0±2.5	0.6
TBDOC–water	216.9±5.1^b	2.2
TBDOC–PG	487.6±41.6^b	5.0
TBDOC–ethanol	44.5±8.4^b	0.4
TBDOC–PEG 400	192.0±7.2^b	2.0

[a] Ratio of J of DEET in presence of treatment to J of DEET in absence of treatment
[b] Statistically different compared to no treatment at 95% confidence interval ($p<0.05$)

Human Stratum Corneum Isolation and Sample Preparation

The SC was separated from the dermis by placing the human cadaver skin sample over a filter paper soaked in 0.1% trypsin (type I, Sigma Aldrich) in phosphate-buffered saline pH 7.4 for 4 h. Epidermal cells were removed from the overlying SC by digestion with trypsin for an additional 1 h. The resulting SC sheets were rinsed with deionized water, dried at room temperature and stored in desiccator overnight. Next day, the SC sheets were mounted on Franz diffusion cell (Permegear, Inc., Bethlehem, PA) set up with their epidermal side up and covered completely with 50 µl of formulations of penetration modifiers prepared in one of the four vehicles for 30 h at 37°C. The penetration modifiers used in the study included laurocapram (1-dodecylazepan-2-one), DMBIS, N-0915, TBDOC, and DMMCBI. The vehicles used in the study included water, propylene glycol, PEG 400, and ethanol. The receptor compartment stirred at 600 rpm contained phosphate-buffered saline at pH 7.4 and was maintained at 37°C using thermostatic water pump (Haake DC10, Karlsruhe, Germany). After 30 h, the SC sheets were removed and excess enhancer/retardant solution present on SC sheets was removed using KimWipes™ (Fisher Scientific, PA). All experiments were performed in triplicate at 37±2°C. SC sheets were then subjected to DSC or ATR-FTIR analysis. Suitable controls experiments were also performed that included untreated SC, treatment with laurocapram alone, water alone, propylene glycol alone, ethanol alone, and PEG 400 alone. Among all the penetration modifiers tested, laurocapram was the only one that existed in liquid state; therefore it was used as one of the controls while comparing laurocapram containing formulations.

Differential Scanning Calorimetry (DSC)

For DSC, approximately 10–20 mg of stratum corneum sheets (treated or untreated) were cut in form of disks and placed in 40-µl aluminum standard pans. Thermal analysis was performed using a STARe/Thermal Analysis System (Mettler-Toledo, Gießen, Germany, DSC 821/822, Intracooler, Gas Switch, 200 W, FRS-5 sensor). All samples were analyzed between 5 and 160°C at 10°C/min heating rate under nitrogen flow.

The mean transition temperatures (T_m) and their corresponding enthalpies were noted and results were evaluated statistically using one-way ANOVA through Minitab software (State College, PA). Tukey HSD test at 95% confidence interval was used to compare the results. The results obtained from the DSC study were correlated with those obtained from *in vitro* permeation findings from our previous study (3).

Attenuated Total Reflectance Fourier-Transform Infra-Red Spectroscopy

FTIR spectra were recorded with a Bruker Equinox 55 spectrometer (100 scans; 4 cm^{-1} resolution), equipped with an attenuated total reflection diamond crystal accessory (Pike Technologies, Madison, WI). Spectra were acquired at a resolution of 4 cm^{-1} and the measurement range was 4,000–650 cm^{-1}. All spectra (100 scans) were collected after baseline correction. The spectrometer was linked to a PC equipped

with Bruker OPUS software to allow the automated collection of IR spectra. The IR spectra were imported to KnowItAll® informatics system (Bio-Rad Lab., USA) for peak area integration. All measurements were performed at ambient temperature, 25±2°C. Like DSC data, findings obtained from ATR-FTIR study were correlated with results from *in vitro* permeation from our previous study (3).

RESULTS

DSC Analysis

Three endothermic transition peaks at temperatures around 59–63°C (T_{m1}), 75–85° (T_{m2}) and 110–120°C (T_{m3}) were obtained on DSC analysis of untreated skin. The temperature and enthalpy changes in DSC of human SC after different formulation treatments are listed in Table II and endotherms of human SC from one of the replicates are depicted in Figs. 1a, 2a, 3a, 4a, 5a, and 6a.

FTIR Analysis

The different spectra depicting different band positions and peak intensities after FTIR analysis of untreated human stratum corneum and treated (after application of various penetration modifier-vehicle formulations) stratum corneum are depicted in Figs. 1b, 2b, 3b, 4b, 5b, and 6b.

DISCUSSION

DSC. Since DSC technique is widely used to investigate the effect of percutaneous penetration enhancers and retardants on the thermotropic behavior of SC (by comparing the endotherms and exotherms for mean transition temperature (T_m) and their enthalpies (H)), it was used to understand the molecular mechanism of each formulation on SC. DSC thermograms of SC treated with various formulations were evaluated by comparing endotherms for ΔT_m and their ΔH. The shift in T_m of both T_{m1} and T_{m2} to lower temperature is interpreted as disruption of the lipid bilayer while reduction in ΔH is ascribed to fluidization of lipid bilayers (13,15,16). DSC of the stratum corneum membrane sheet produced three endothermic transition peaks at temperatures around 59–63°C (T_{m1}), 75–82°C (T_{m2}) and 99.5–120°C (T_{m3}). Three replicates were performed with human cadaver skin obtained from three different individuals; therefore some variability was obtained in the position of three transitions. The temperature transitions and enthalpy changes after several treatments are provided in Table II. We did not observe a commonly reported low transition temperature peak (at 35–40°C) (17) because our SC samples were desiccated before DSC analysis and 15% moisture content is required for observation of low temperature transition (18). Moreover, Golden *et al.* (16) attributed the variable nature of the endothermic transition at 35–40°C to sebaceous lipids that are not tightly bound with the SC surface and have little influence on the ordering of the SC. T_{m1} corresponds to the lipid transformation from a lamellar to disordered state. Similarly, T_{m2} is thought to be due to the melting of lipid–protein (keratin) complex that transitions from a gel to a liquid form during DSC analysis (19). T_{m3} is known to occur

Table II. Mean Temperature Shifts and Enthalpy Change of SC After Treatment with Laurocapram, Laurocapram Analogues and Iminosulfurane Formulations

Treatments	Mean temperature shift (°C)±SD ($n=3$)			Mean enthalpy change (J/g)±SD ($n=3$)		
	ΔT_{m1}	ΔT_{m2}	ΔT_{m3}	ΔH_1	ΔH_2	ΔH_3
No treatment	–	–	–	–	–	–
Water	-3.0 ± 0.8^a	-6.2 ± 1.7^a	-1.5 ± 0.14^a	-0.01 ± 0.001	-0.03 ± 0.02	-0.008 ± 0.003^a
PG	-2.0 ± 0.9^a	-6.0 ± 4.5^a	$–^b$	0.4 ± 0.01	0.5 ± 0.01	$–^b$
Ethanol	-14.0 ± 0.01	-6.0 ± 4.0^a	$+8.5\pm0.04$	0.4 ± 0.04	0.4 ± 0.09	0.02 ± 0.001
PEG 400	$+7.0\pm2.2^a$	$+2.0\pm5.5^a$	$–^b$	0.1 ± 0.03^a	0.1 ± 0.01	$–^b$
Laurocapram	$–^b$	-13.1 ± 0.9^a	$–^b$	$–^b$	0.1 ± 0.02	$–^b$
Laurocapram–water	$–^b$	$–^b$	-7.5 ± 1.0^a	$–^b$	$–^b$	-0.05 ± 0.01
Laurocapram–PG	-9.0 ± 4.2^a	$–^b$	-7.5 ± 5.4^a	0.05 ± 0.001	$–^b$	0.5 ± 0.04
Laurocapram–ethanol	-5.0 ± 1.9^a	$+2.0\pm0.8^a$	-9.9 ± 0.7^a	-0.6 ± 0.05	-0.8 ± 0.3	No change
Laurocapram–PEG 400	-5 ± 1.6	No change	$–^b$	0.7 ± 0.05	-0.1 ± 0.01^a	$–^b$
N-0915–water	$–^b$	Merger of T_{m1} and T_{m2} at 70°C	Multiple peaks at 92, 94 and 100°C	$–^b$	–	–
N-0915–PG	-3.0 ± 1.6	-7.0 ± 0.5^a	-6.5 ± 1.4	0.7 ± 0.04	-0.1 ± 0.03	1.4 ± 0.4^a
N-0915–ethanol	$+9.0\pm1.3^a$	$+8.0\pm0.03^a$	$+8.5\pm0.9$	-0.4 ± 0.02	-1.0 ± 0.2	No change
N-0915-PEG 400	$+6.0\pm0.4^a$	$+1.0\pm0.3^a$	$–^b$	No change	No change	$–^b$
DMBIS–water	-3.0 ± 1.5^a	-8.0 ± 3.7^a	-9.9 ± 0.09^a	-0.9 ± 0.3	-0.7 ± 0.03	0.02 ± 0.008
DMBIS–PG	-4.3 ± 1.2^a	-10.0 ± 0.8^a	-13.5 ± 4.9^a	1.0 ± 0.6	0.01 ± 0.01	0.01 ± 0.06
DMBIS–ethanol	No change	No change	$–^b$	No change	No change	$–^b$
DMBIS–PEG 400	$+3.0\pm1.4^a$	$+2.0\pm3.1^a$	$+22.5\pm4.0^a$	0.29 ± 0.04	-0.06 ± 0.01	0.3 ± 0.01
DMMCBI–water	-1.0 ± 0.05	-8.0 ± 3.0	$-3.5\pm.5$	0.05 ± 0.01	0.2 ± 0.01	-0.01 ± 0.002
DMMCBI–PG	-3.0 ± 0.5^a	-7.0 ± 2.0^a	$–^b$	0.25 ± 0.06	-0.24 ± 0.02	$–^b$
DMMCBI–ethanol	-9.0 ± 0.04	Two peaks at 84°C and 88°C	$–^b$	0.7 ± 0.3	–	$–^b$
DMMCBI–PEG 400	$+6.0\pm0.5$	$+2.0\pm0.6$	$–^b$	0.4 ± 0.03	-0.07 ± 0.01	$–^b$
TBDOC–water	-9.0 ± 1.6	-10.0 ± 2.0^a	$–^b$	No change	0.01 ± 0.001	$–^b$
TBDOC–PG	$–^b$	Merger of T_{m1} and T_{m2} at 70°C	$–^b$	$–^b$	–	$–^b$
TBDOC–ethanol	$+9.0\pm0.8^a$	$+12.0\pm0.4^a$	$+4.5\pm0.08^a$	0.3 ± 0.09	-0.8 ± 0.1	No change
TBDOC–PEG 400	No change	No change	$–^b$	0.5 ± 0.03	-0.01 ± 0.005	$–^b$

SD standard deviation
[a] Statistically different compared to no treatment at 95% confidence interval ($p<0.05$)
[b] Missing peak

due to the irreversible denaturation of proteins in the SC (20). DSC was also performed on suitable controls that included SC treated with the following different treatments: water, PG, ethanol, PEG 400, and laurocapram. The DSC data of stratum corneum treated with water showed lowering of mean transition temperature transitions and lowering of heat of enthalpy suggesting enhancement of the active by water, by SC lipid disruption, and by extraction. This observation also implies that water causes transdermal enhancement either by expanding the polar head groups of SC lipid bilayer or by squeezing and distorting the lipid bilayer by swelling/engorgement of the corneocytes (9). However, these explanations of water enhancement are contradicted by studies performed on hydrated SC using X-ray diffractometry (21) and freeze fracture electron microscopy (22) that reported neither expansion of lipid bilayer, nor distortion of lipid bilayer in hydrated skin. At the same time, Menon *et al.* (23) proposed an aqueous pore pathway for the diffusion of actives across the skin under high stress conditions such as excessive hydration. According to this theory, under conditions such as excessive hydration, pre-existing scattered lacunae embedded in the lipid bilayer expand and form continuous water channels that facilitate diffusion of both hydrophilic and lipophilic permeants. This may also suggest that formation of these aqueous pathways disrupt the surrounding lipid bilayer as shown by change in transition temperatures and enthalpy seen in our DSC results. PG is thought to cause enhancement predominantly by disturbance of lipid–protein complex and the interaction with lipids shown by lowering of T_{m1} ($p<0.05$) and T_{m2} ($p<0.05$). Like PG, the thermal analysis of ethanol-treated SC suggested enhancement is mainly due to disturbance of SC lipid–protein complex and SC lipid interactions. In case of PEG 400, thermal analysis showed increase in first and second transition temperatures and increase of enthalpy indicating the strengthening of SC lipids organization and SC lipid–protein complex after treatment with PEG 400. This observation explains the retardation of DEET permeation after PEG 400 treatment (3). The treatment of SC with laurocapram alone led to complete extraction of lipid at T_{m1} and T_{m3} with significant lowering of endothermic transition at T_{m2}. All these observations suggest enhancement by laurocapram via both lipid disruption in addition to protein and lipid extraction. This finding is corroborated by results reported by Ogiso *et al.* (24).

Laurocapram Formulations. DSC analysis of SC treated with laurocapram–water showed disappearance of T_{m1} and T_{m2} transitions and significant lowering of the temperature
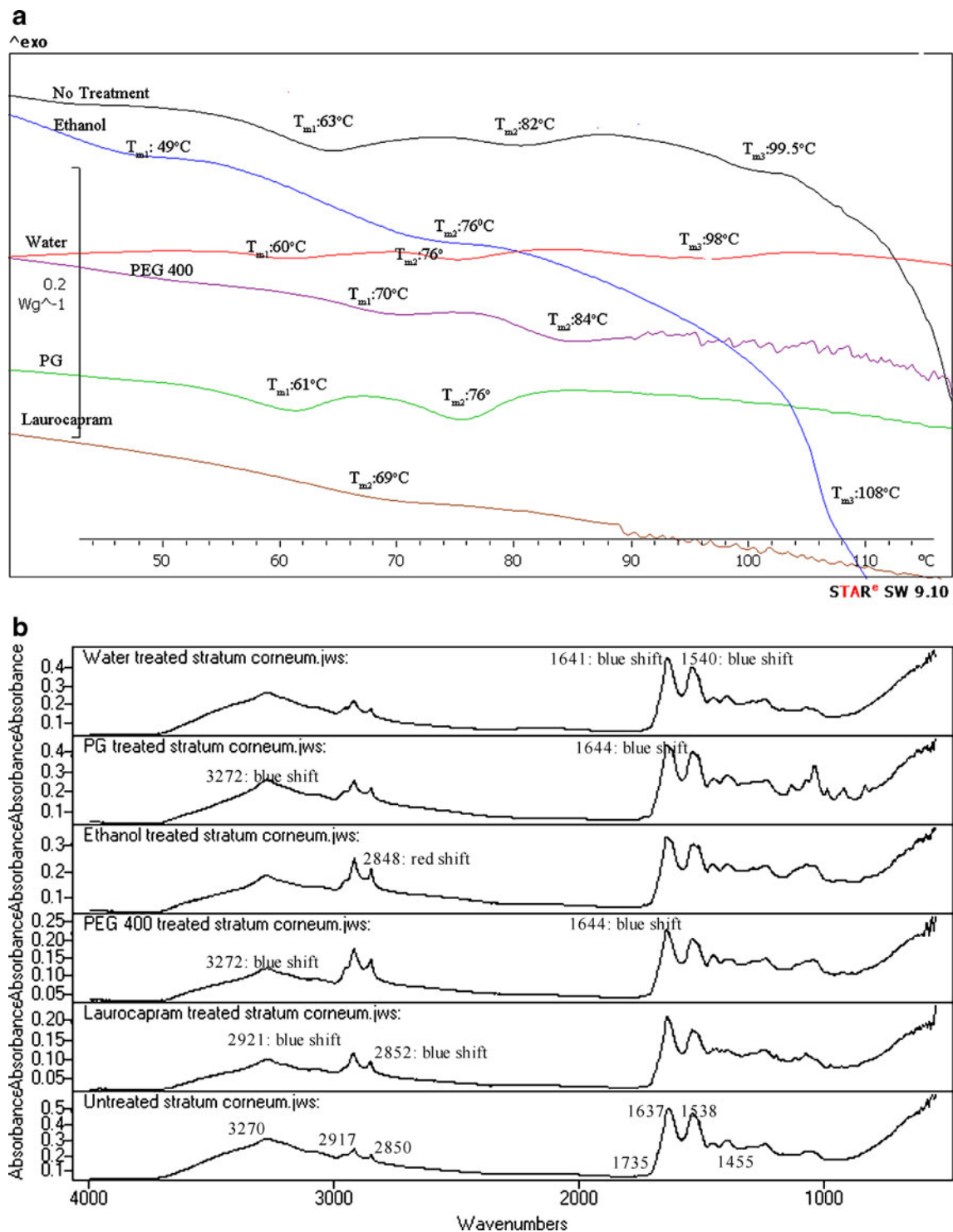
Fig. 1. a DSC of untreated human SC and SC treated with selected vehicles. **b** IR spectra of untreated human SC and SC treated with selected vehicles

transition at T_{m3} ($p < 0.05$) with some lowering of the enthalpy at the T_{m3} transition. These results imply that laurocapram and water in the formulation contribute to enhancement by lipid disruption, lipid extraction, and protein denaturation. This also explains the increased flux of DEET after treatment with laurocapram–water formulations as compared to controls (3).

In the laurocapram–PG formulation, there was a lowering of T_{m1} ($p < 0.05$) and T_{m3} ($p < 0.05$) peaks and disappearance of

T_{m2} indicating that laurocapram–PG causes lipid disruption, lipid and protein extraction. The laurocapram and PG present in laurocapram–PG formulation contributes to lipid and protein disruption in the SC and also lead to complete extraction of lipid–protein complex. Both laurocapram and PG act in synergy to increase the permeability of the SC as shown by increased flux of DEET in presence of laurocapram–PG (25).
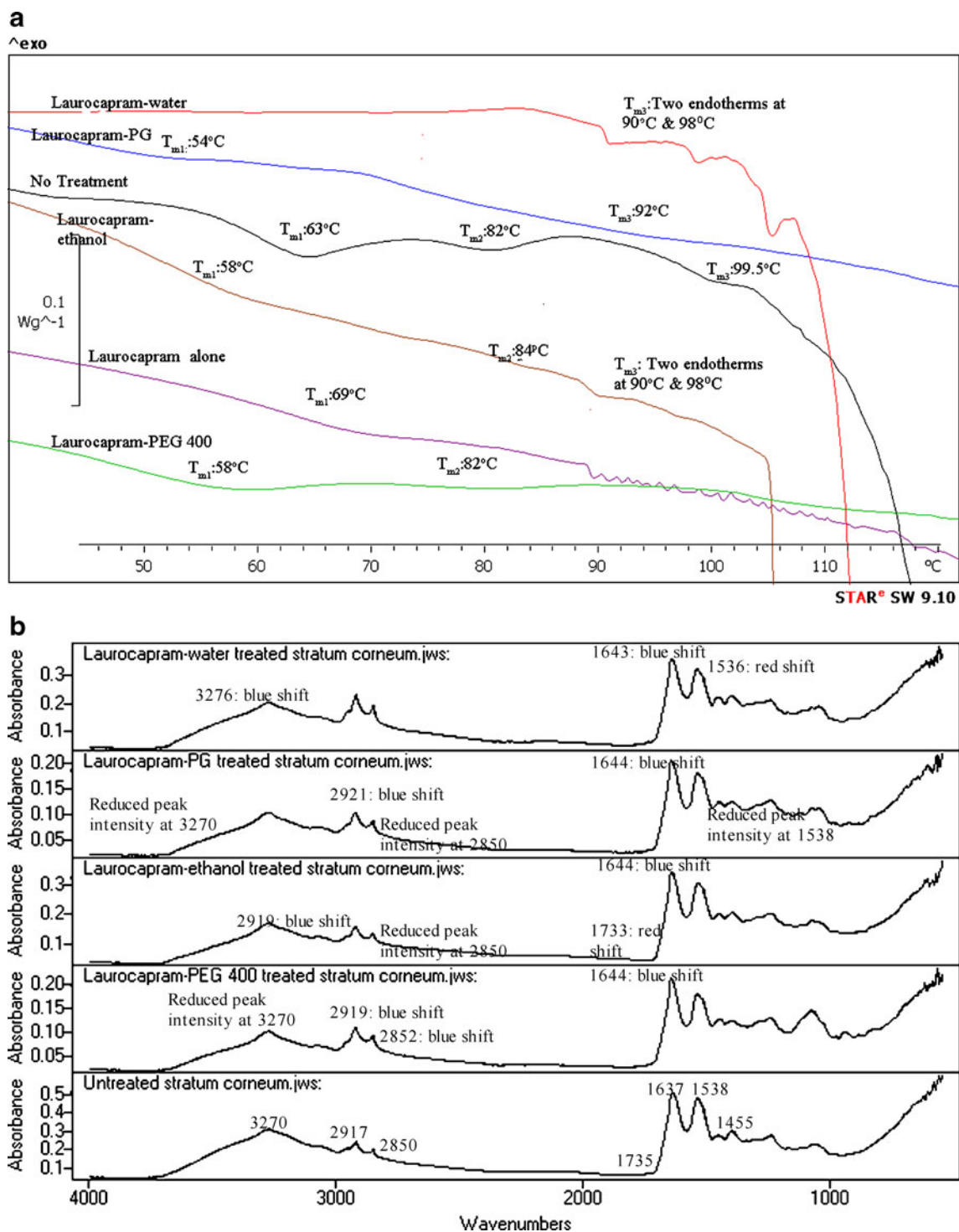
Fig. 2. a DSC of untreated and laurocapram-formulations-treated human SC. **b** IR spectra of untreated and laurocapram-formulations-treated human SC

As with PG, the DSC results suggested enhancement of active after treatment with laurocapram–ethanol formulation was due to lipid extraction, lipid and protein extraction shown by significant lowering of temperature at T_{m1} and T_{m3} transitions (except T_{m2}) ($p<0.05$) and ΔH. One interesting feature that was observed in DSC thermogram on application of laurocapram–ethanol formulation was that there was elevation at T_{m2} transition. Ethanol, when incorporated with

other enhancers such, has 0.25% oleic acid has shown similar behavior of elevation in transition temperature in DSC experiments. Studies performed by Francoeur *et al.* (26) showed elevation in second lipid endotherm in porcine SC after treatment by 0.25% *v/v* oleic acid formulations prepared in 0–70% ethanol–water vehicles. However, the reason for this phenomenon is not known. In our study, though the laurocapram–ethanol formulation had 88% of ethanol, never-
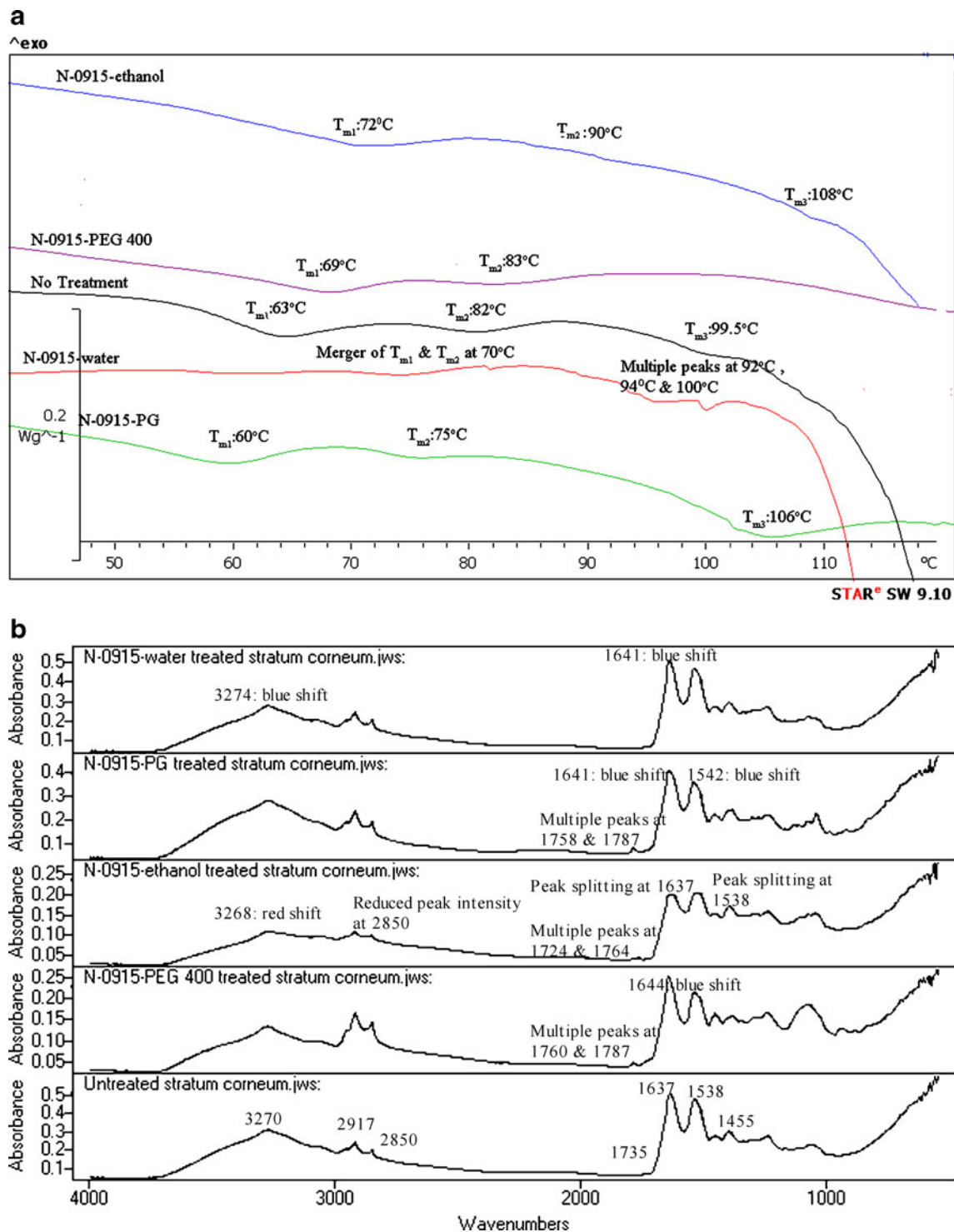
Fig. 3. a DSC of untreated and N-0915-formulations-treated human SC. b IR spectra of untreated and N-0915-formulations-treated human SC

theless there was elevation in the second lipid endotherm of SC treated with laurocapram–ethanol formulation.

In laurocapram–PEG 400 formulation, DSC data showed decrease in T_{m1} transition temperature, no change in T_{m2} and disappearance of T_{m3}. It seems that laurocapram and PEG 400 in laurocapram–PEG 400 formulation tend to cause opposite effect on SC with laurocapram causing disruption of lipid and proteins in the SC (T_{m1} and T_{m3}) and PEG 400

causing strengthening of lipid–protein complex evident by no change in T_{m2}. This observation supports the results observed in the *in vitro* permeation experiment where the laurocapram–PEG 400 formulation retarded the permeation of DEET (3). The *in vitro* permeation studies comparing flux of DEET in presence of laurocapram–PEG 400 and PEG 400 alone have indicated that incorporation of laurocapram in the formulation increased the flux of DEET as compared to
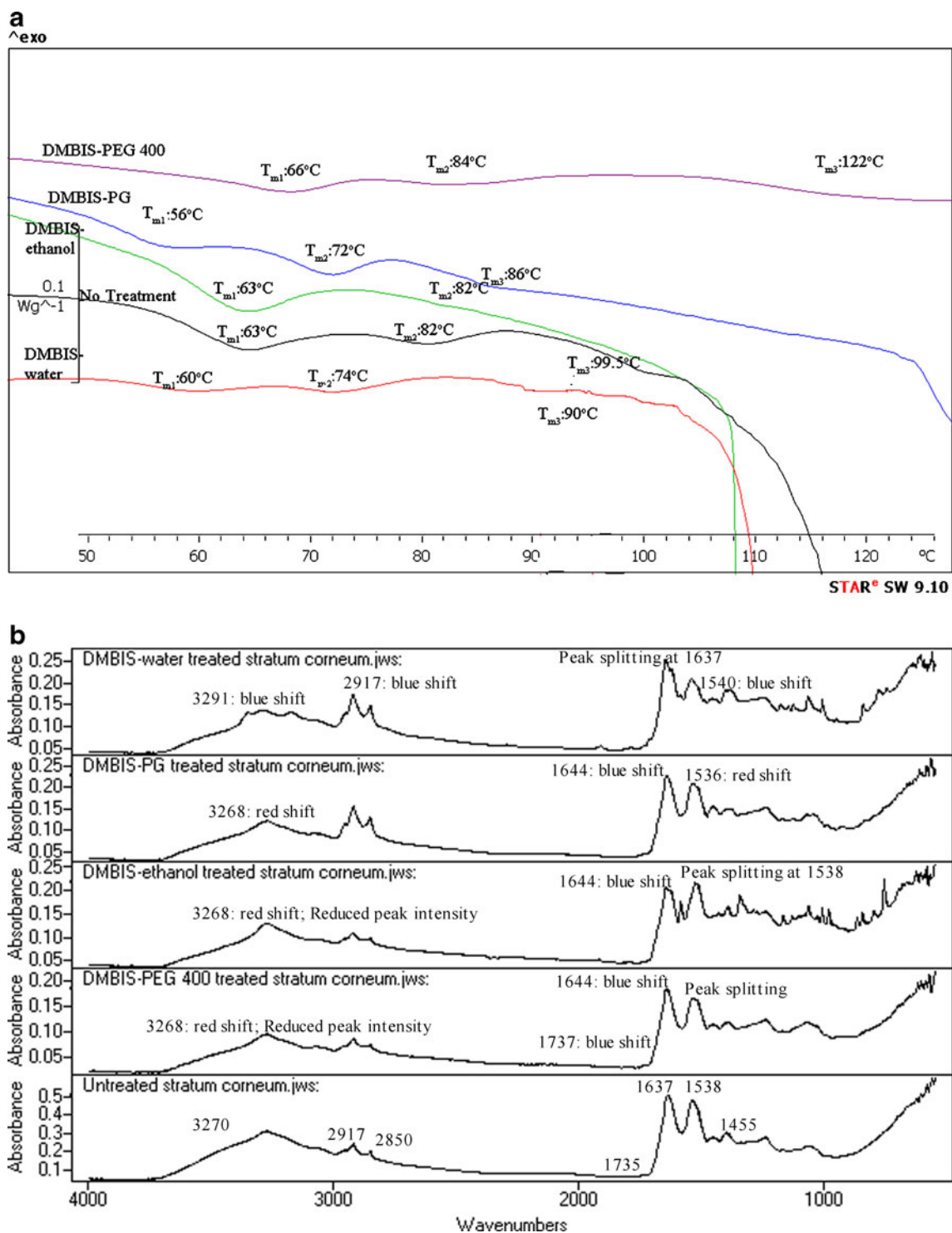
Fig. 4. **a** DSC of untreated and DMBIS-treated human SC. **b** IR spectra of untreated and DMBIS-treated human SC

treatment with PEG 400 alone (3). Similarly, on comparison of DEET permeation in presence of laurocapram–PEG 400 and laurocapram alone showed that DEET permeation in presence of laurocapram was higher than in presence of laurocapram–PEG 400 (3). Nevertheless, other analytical techniques such as confocal Raman spectroscopy (27,28), X-ray diffractometry (29), *etc*., should be investigated in addition to DSC, that would not only measure the extent of

permeation of the actives/penetration modifiers across the SC, but also determine the corresponding effect of the formulations (under study) on SC lipids and proteins. This would also help us to establish whether PEG 400 retards the activity of the permeant physically (by forming a barrier layer) or by its interaction with SC lipids and proteins or both. However, in our study, beside DSC, FTIR was also used to understand the mechanism of action of each formulation.
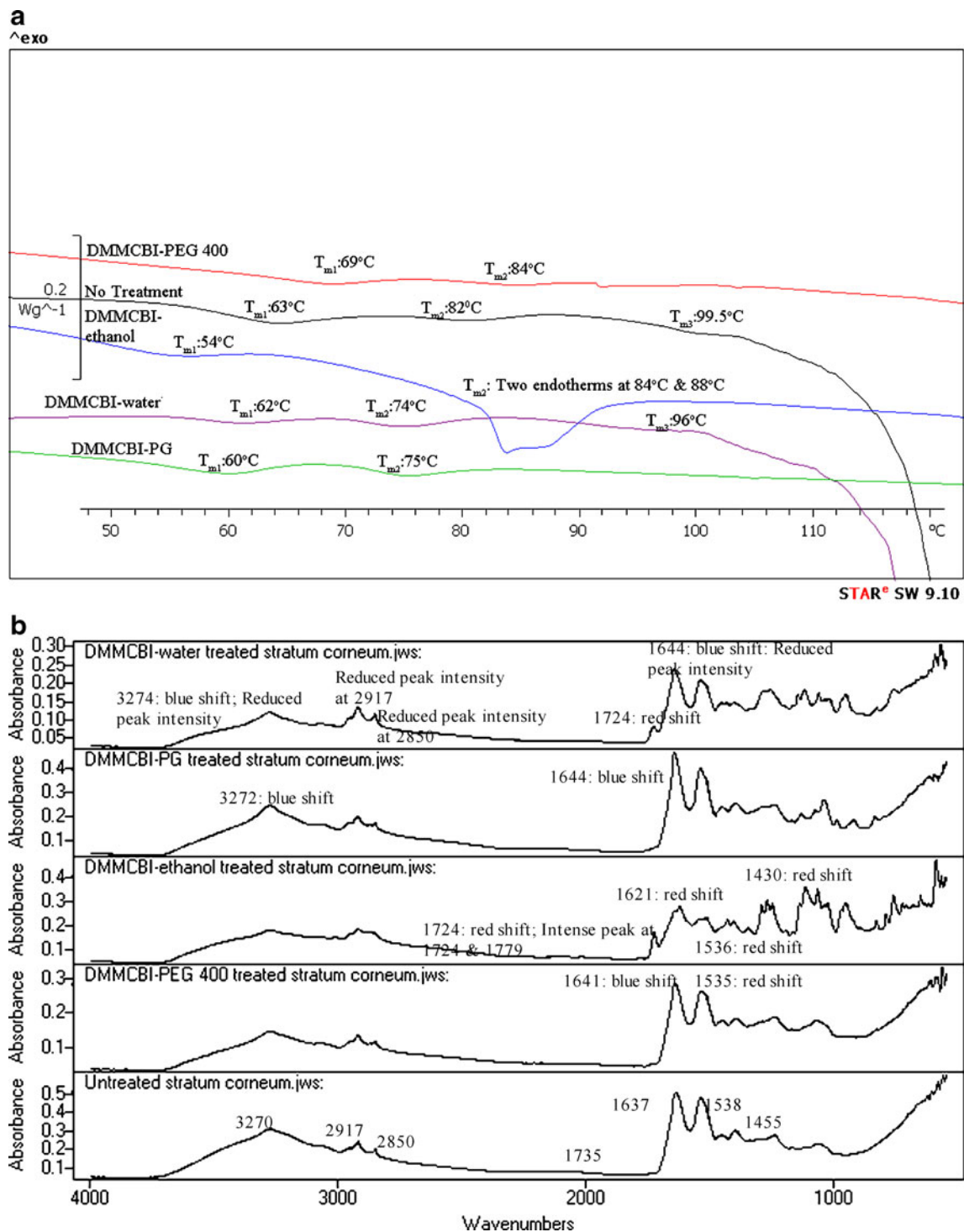
Fig. 5. **a** DSC of untreated and DMMCBI-treated human SC. **b** IR spectra of untreated and DMMCBI-treated human SC

N-0915 Formulations. DSC analysis of N-0915–water showed merger of T_{m1} and T_{m2} at 70°C and multiple peaks at 92, 94, and 100°C suggesting of lipid fluidization of SC lipids. Mean flux determination of DEET after N-0915–water produced enhancement of DEET as compared to control (3), a finding that agrees with conclusions from the DSC results.

DSC results in N-0915–PG treatment showed lowering of T_{m1}, T_{m2}, and T_{m3}. However, results in our previous *in vitro* permeation study suggested retardation of DEET permeation

after N-0915–PG application (3). It seems that N-0915–PG retardation cannot be explained using DSC and alternate approach such as FTIR was performed.

In N-0915–ethanol treatment, flux determination of DEET indicated retardation of DEET as compared to control (3), an observation that agrees with our DSC results. N-0915–ethanol formulation seems to cause retardation of active by organization of lipid structure evident by increase in ΔT_{m1} ($p < 0.05$), strengthening the lipid–protein complex shown by
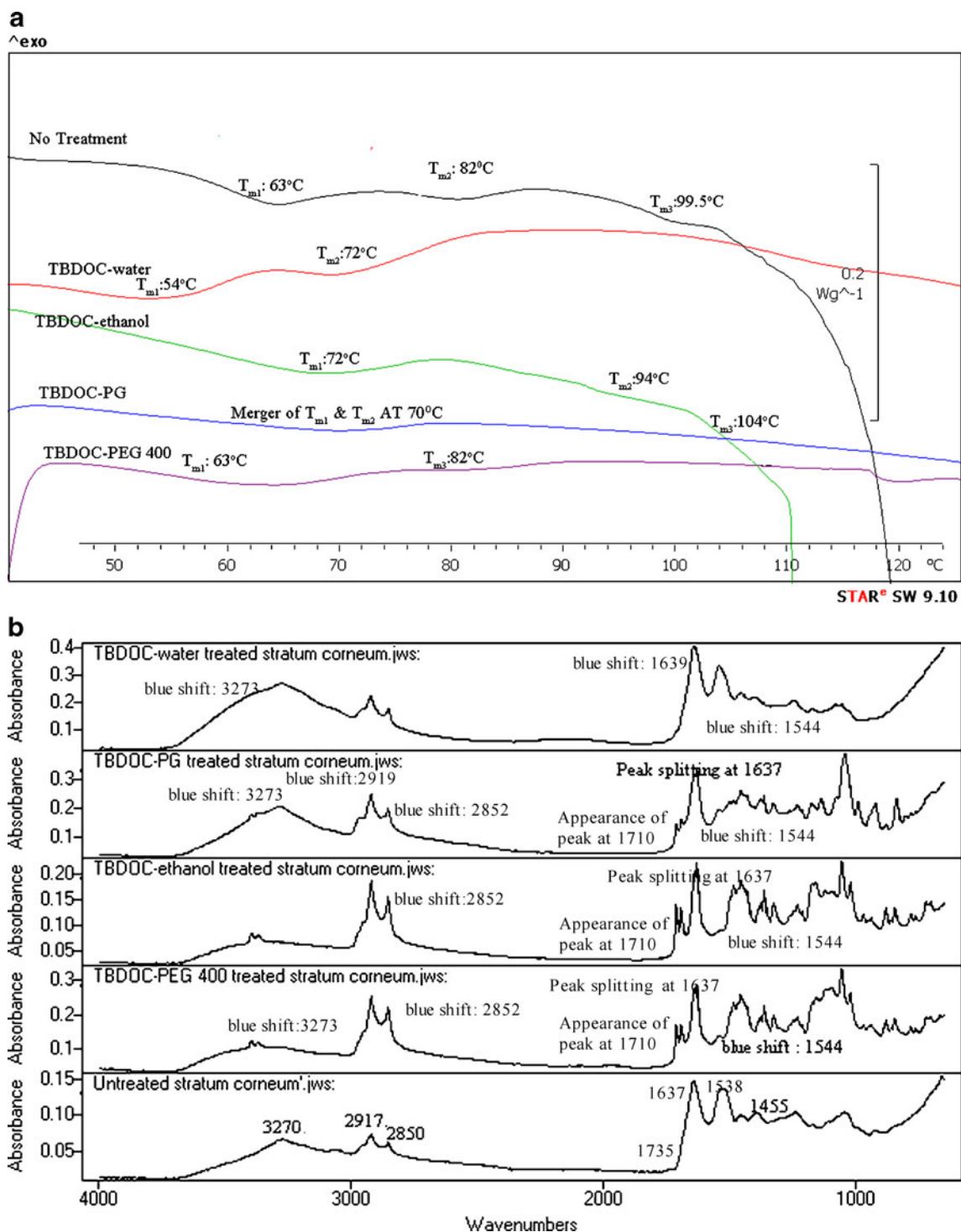
Fig. 6. **a** DSC of untreated and TBDOC-treated human SC. **b** IR spectra of untreated and TBDOC-treated human SC

higher shift of T_{m2} ($p<0.05$) and organization of proteins to a higher temperature (evident by higher ΔT_{m3}). However, lowering of ΔH was seen at most transition temperatures.

Likewise, N-0915–PEG 400 showed retardation of DEET (3) by organization of lipids (evident by higher shift in T_{m1}) and strengthening of the lipid–protein envelope (suggested by increase in T_{m2}) of SC. There was no enthalpy change at all the corresponding transition temperatures.

DMBIS Formulations. DMBIS–water-treated SC showed lowering of shifts at T_{m1} ($p<0.05$), T_{m2} ($p<0.05$), T_{m3} ($p<0.05$) indicating that enhancement is probably caused by lipid disruption and protein interactions. Slight effects of DMBIS–water were seen on lipid extraction as evidenced by insignificant changes in enthalpy of lipids at each transition. DSC results support the enhancement in permeation of DEET in the presence of DMBIS–water (3).

DMBIS–PG formulation seemed to cause significant lowering of T_m transitions ($p < 0.05$) that suggests enhancement caused by lipid and protein disruption. These results may explain the approximate threefold enhancement of DEET flux as compared to controls (3).

DSC analysis of DMBIS–ethanol-treated SC depicted no change in T_{m1} and T_{m2} transition but disappearance of T_{m3} endotherm explaining slight enhancement in DEET permeation after treatment with DMBIS–ethanol in *in vitro* experiments (3). The enhancement activity by DMBIS–ethanol treatment seems to be due to extraction of proteins.

Like other DMBIS formulations, DMBIS–PEG 400 showed enhancement of DEET permeation (3). However, DSC analysis of DMBIS–PEG 400-treated SC showed higher ΔT at all three temperature transitions. Owing to the inconsistent results from *in vitro* permeation study and DSC, FTIR analysis was performed to understand the mechanism of action of DMBIS–PEG 400.

DMMCBI Formulations. DMMCBI–water formulation showed lowering of mean transition temperature at T_{m1}, T_{m2}, and T_{m3} with some lowering of enthalpy at T_{m3}. These results imply enhancement in presence of DMMCBI–water formulation which explains the enhancement of DEET in presence of DMMCBI–water formulation. DMMCBI–water formulation seems to cause enhancement by lipid disruption and protein fluidization.

In DMMCBI–PG, we observed significant lowering of mean transition temperature ($p < 0.05$) at all transitions with lowering of enthalpy as compared to untreated SC at T_{m2}. These results suggest enhancement by DMMCBI–PG formulation mainly by lipid disruption and partially by lipid and protein fluidization.

Thermal analysis of DMMCBI–ethanol-treated SC showed lowering of transition temperature at T_{m1} ($p > 0.05$), two peaks at 84°C and 88°C at T_{m2} with disappearance of T_{m3} transition. *In vitro* permeation studies showed significant retardation in presence of DMMCBI–ethanol ($p < 0.05$) (3) suggesting retardation action of DMMCBI–ethanol formulation by interaction at lipid–protein complex.

In vitro permeation studies of DEET in presence of DMMCBI–PEG 400 indicated slight retardation of the permeant (3). However, DSC analysis of SC treated with DMMCBI–PEG 400 showed significant increase in temperature shifts at T_{m1}, T_{m2} and disappearance of peak at T_{m3}. This suggests organization of lipid structure as well as strengthening of lipid–protein complex in presence of DMMCBI–PEG 400.

TBDOC Formulations. In TBDOC–water-treated SC, DSC showed lowering of T_{m1} and T_{m2} ($p < 0.05$) with absence of T_{m3} transition. At the same time, *in vitro* flux determination of DEET in presence of TBDOC–water formulation showed a twofold increase in flux as compared to no treatment (3). The enhancement of DEET in presence of TBDOC–water seems to be due to disruption of the lipid with little effect on lipid fluidization.

TBDOC–PG application on human cadaver skin led to fivefold increase in DEET flux (3). DSC analysis of SC treated with TBDOC–PG showed merger of T_{m1} and T_{m2}

transition at 70°C and disappearance of peak at T_{m3}. These results suggest enhancement in presence of TBDOC–PG was caused by disruption of the lipid–protein complex with fluidization and extraction of certain SC lipids and proteins.

Analysis of TBDOC–ethanol formulation showed significant increase ($p < 0.05$) in shifts at T_{m1}, T_{m2}, and T_{m3} indicating strengthening of SC lipid bilayer suggesting the role of TBDOC in the ethanol formulation as a retardant. This finding is corroborated by *in vitro* permeation study where significant retardation of DEET was observed in the TBDOC–ethanol formulation.

In TBDOC–PEG 400-treated SC, no change was obtained in temperature transitions at T_{m1} and T_{m2}. However, decrease in ΔH at T_{m2} and disappearance of endotherm at T_{m3} suggested enhancement by extraction of SC lipid–protein complex and SC protein extraction suggesting. The *in vitro* permeation study indicated twofold enhancement in flux of DEET after TBDOC–PEG 400 formulation (3).

It appeared that enhancement/retardation of formulations under investigation could not be explained by DSC alone in certain cases, therefore SC treated with all formulations were also assessed by FTIR analysis.

FTIR. The FTIR analysis of SC provides bands at different wavenumbers, which are attributed to lipid and protein molecular vibrations in the SC (30,31). In our study, untreated human SC showed bands at 3270.7, 2917.8, 2850.3, 1735.6, 1637, 1538.9, and 1455.9 cm^{-1}. Among these bands, the signal around 3270 cm^{-1} represents symmetric H–O–H stretching and overlaps with an amide A band located at 3300 cm^{-1} position. Generally, the bands observed in range of 3000–3600 cm^{-1} represent the N–H and O–H stretching from lipid, protein, and water. The prominent peaks obtained near 2920 and 2850 cm^{-1} represented respectively asymmetric and symmetric stretching modes of the terminal methylene groups of the lipids (ceramides, phospholipids, *etc.*) that provided specific information about the interior composition of the lipid bilayer. The ceramides along with cholesterol, fatty acids, cholesterol esters, and cholesterol sulfate constitute the multiple lipid lamellae that impart barrier properties to SC. The SC also contains corneocytes that contain keratin. The band positions for symmetric and asymmetric peak stretching represent trans form (stable form); change in the band position from trans to gauche conformation indicates the fluidization of the lipid bilayer (32). A small band obtained at 1738 cm^{-1} position represented lipid ester carbonyl stretching in the SC. Spectral deconvolution techniques have shown that the band shape at 1738 cm^{-1} can be simulated with two band components at 1740 and 1710 cm^{-1} with the former, indicating the presence of carbonyl moiety as in triglycerides/phospholipids and the latter suggesting the presence of carbonyl group of fatty acids (33,34). The bands observed near 1637 and 1550 cm^{-1} represented amide 1 (C=O stretching) and amide 2 (C–N stretching) linkages of the helical secondary structure found in epidermal keratin (35). Besides absorbance due to protein structure, amide linkages in ceramides and other related components in the SC also contribute to amide 1 band (36,37). However, the presence of protein contributes more to the appearance of signal at this band position. Along with amide 1 band, another peak is reported around 1645 cm^{-1} that corresponds to H–O–H

bending. The amide bands along with 1645 cm^{-1} band are known to be sensitive to H-bond change in the SC. In our experiment, there was overlapping of the 1645 cm^{-1} and 1655 cm^{-1} peaks in untreated human SC sample that led to appearance of a single intense peak at 1637 cm^{-1} that was regarded as amide 1 linkage of the proteins and lipids. The SC lipids can be examined by the investigation of the band representing lipid alkyl backbone through the CH$_2$ scissoring (1462–1474 cm^{-1}) that are indicators of lateral packing within the lamellae. A single methylene band at ~1468 cm^{-1} represents hexagonal acyl chain packing of the lipids whereas orthorhombic chain packing is indicated by two components at 1472 cm^{-1} and 1464 cm^{-1}. Triclinic chain packing is known to give a single band ~1473 cm^{-1} [38].

In our study, SC sheets were treated with various formulations of penetration modifiers for a period of 30 h at 37°C followed by spectral analysis by ATR-FTIR. Spectral analysis involved examination of change in peak positions and their intensities at around 3270.7, 2917.8, 2850.3, 1735.6, 1637, 1538.9, and 1455.9 cm^{-1} with respect to the control (untreated) SC (Fig. 1b). The spectral data were used to understand the enhancement/retardation mechanism of the penetration modifiers (laurocapram, N-0915, DMBIS, DMMCBI, and TBDOC) formulated in commonly used vehicles (water, PG, ethanol, and PEG 400). The rationale for use of FTIR technique to understand mechanism of penetration modifier was that the treatment with enhancers/retardants, sometimes yield a shift in specific band position to higher or lower wavenumber or lead to change in the intensity of the signal observed at that band position. If the shift is to higher wavenumber (blue shift) it signifies SC membrane (lipid bilayer) fluidization that in turn leads to disruption of the barrier properties that thereby causes enhancement of the permeation of the active across the SC [39,40]. On the other hand, a shift to lower wavenumber (red shift) indicates reorientation of lipid groups leading to strengthening of the SC barrier properties and therefore leads to retardation of the entry of permeant across the skin [41,42]. If the penetration modifier acts by affecting lipoidal pathway, the phase transition of the lipids is represented by increase/decrease in the band position (wavenumber) of the signals at 2920, 2850, and 1738 cm^{-1}. Similarly, when penetration modifiers affect the ceramides of the SC at the amide 1 signal, a decrease in wavenumber (red shift) is indicative of strong H-bonding with the ceramide 2 molecules [43–45]. On the other hand, an increase in the wavenumber at 1537 cm^{-1} position (blue shift) is indicative of strong hydrogen bonding interactions within the stratum corneum ceramides [44]. The change in protein conformation is also reflected by splitting of amide 1 linkage where there is change from alpha helix secondary structure to beta helix structure of keratin and *vice versa* [36].

Since the height or area of the bands represents the amount of lipids/proteins in the SC, any change in the peak intensity suggests the extraction or strengthening of the lipid present in the SC. The treatment with penetration modifiers may lead to extraction of the membrane lipids from the SC as in the case of enhancers, or might increase the intensity at particular band representing retardation in the case of retardants.

Laurocapram Formulations. The spectral analysis of laurocapram–water-treated SC suggests that water compo-nent of the formulation caused enhancement by increased water partitioning into the hydrated keratin fibrils of SC (evident by 3270 and 1637 cm^{-1} blue shifts) and laurocapram contributed to the phase transition of the ceramides of the SC (blue shift at 1637 cm^{-1}) [44]. We observed that laurocapram alone actually caused shift in the wavenumber of the symmetric (2917.8 cm^{-1}) and the asymmetric (2850 cm^{-1}) bands [32], but there was no effect of on these bands in the laurocapram–water formulation. The results suggest that laurocapram alone caused enhancement via lipid fluidization and lipid extraction indicated by a marked decrease in lipid content in SC at all bands shown by blue shifts observed at certain frequencies. These spectral results explain the fourfold flux enhancement of DEET in presence of laurocapram–water formulation [3].

The spectra of laurocapram–PG-treated SC suggests that PG present in laurocapram–PG formulation contributes to enhancement by changing the conformation of proteins (formation of distorted beta structures) or lipids (breaking of H-bonds of the ceramides) of the SC [44]. Moreover, laurocapram causes phase transition of the lipids [46]. There was significant decrease in peak height at 3270, 2917, 2850, 1538 cm^{-1} in the laurocapram–PG formulation, suggesting lipid extraction by the laurocapram–PG. These observations also support synergistic effects of PG and laurocapram combinations in disturbing the SC barrier properties and thereby causing enhancement of the active. This phenomenon has been reported by other researchers [25].

The ethanol in the laurocapram–ethanol formulation contributed to enhancement mainly by SC lipid extraction, whereas laurocapram present in the formulation caused enhancement by SC lipid extraction, lipid phase transition and fluidization. Ethanol-alone treatment, on spectral analysis, showed a red shift at 2850 cm^{-1} suggesting lipid ordering effect of the solvent that is consistent with observations by Bommannan *et al.* [47] and other researchers in both *in vitro* and *in vivo* experiments [47,48]. This evidence of lipid ordering in presence of ethanol on spectral analysis is contradictory to our DSC result where ethanol-treated SC showed lowering of transition temperature suggesting enhancement by affecting the SC lipids. Like our FTIR results [47,48], DSC results were also consistent with numerous reports that involved DSC of ethanol-treated SC [42,49]. It seems that affect observed on SC lipids in our DSC experiments (that involved lowering of transition temperature) was due to extraction of lipids from the bilayer. At the same time, it appears that in spite of the extraction of lipids, there was no change in the mobility or conformation of lipid which was evident by the red shift seen in the IR spectrum of ethanol-treated SC. Therefore, the enhancement of DEET that was observed in our previous study [3] following ethanol treatment was probably due to extraction of lipids present in the SC.

Laurocapram–PEG 400 formulation showed blue shift at 2917 cm^{-1}, 2850 cm^{-1}, and 1735.6 cm^{-1} band positions on spectral analysis. These band shifts suggest enhancement of permeant as opposed to the retardation of DEET observed in our *in vitro* permeation studies. No change in band intensity or band position was observed at any other band position. This observation is not consistent with our DSC data that

suggested retardation of the permeant after treatment with laurocapram–PEG 400 formulation. This emphasizes the need for use of additional analytical techniques that will not only determine penetration modifier uptake, but also the interactions with SC lipids and proteins. The retardation of DEET in presence of laurocapram–PEG 400 was presumably due to the fact that laurocapram–PEG 400 prevented the partitioning of DEET into the skin resulting in reduced permeation. Wotton *et al.* made a similar observation, a test solution of 1% laurocapram and 18% PEG 400 decreased the permeation of metronidazole across the SC (50).

N-0915 Formulations. The spectral analysis of N-0915–water-treated SC (Fig. 3b), suggest enhancement may be due to increased partitioning of water from the N-0915 formulation into the SC with formation of aqueous pores (23) in the SC affecting the alpha helical keratin structure along with lipid interactions (ceramides/triglycerides) shown by a band shift at 1641 cm^{-1} (44). This is suggestive of increased enhancement of DEET *in vitro* permeation in presence of N-0915–water formulation (3).

In N-0915–PG-treated SC, a blue shift was observed at 1735 cm^{-1} band position with marked increment in the peak intensity representing the increase organization of triglycerides molecules or other lipid components (31,35) present in the SC. The increase in peak intensity was due to the presence of N-0915 in the formulation since the increase was absent in the spectrum obtained from PG-alone-treated SC. The blue shift in the amide 2 band suggests the formation of a strong H-bond within the ceramide molecules (44), and hence strengthening of the barrier function of SC. The spectral changes observed are in agreement with retardation of DEET observed in presence of N-0915–PG in the *in vitro* permeation experiment (3). Moreover, ATR-FTIR technique proves to be a suitable alternative as compared to DSC to explain the mechanism of surface modification of SC by enhancers/retardants.

In N-0915–ethanol, SC spectral analysis showed a red shift at 3270 cm^{-1} position with no change in peak intensity at this position. The red shift indicates possible dehydration of SC. Also N-0915–ethanol-treated SC showed two intense bands at 1724 and 1764 cm^{-1} suggesting reorganization of the head groups of triglycerides or ceramides in the SC to form a tighter structure (51). Furthermore, in comparison to 1736 cm^{-1} band, a relative red shift was observed at 1724 cm^{-1} indicating formation of strong hydrogen bonds within the lipid molecules. Band splitting at 1637 and 1538 cm^{-1} was also observed that may be due to interlamellar vibrational coupling between amide groups of ceramide 2 molecules of the SC (43). Moreover, reduced peak intensity at 2850 cm^{-1} was observed that may be related to extraction of lipid due to presence of ethanol in the formulation. It appears that the dehydration effect (52), along with the organization of SC lipids following application of N-0915–ethanol caused more impact than lipid extraction, an effect that ultimately led to the retardation action of the formulation. Levang reported that dehydration causes keratins of the SC to shrink, which ultimately decreases skin permeability (53). Thus, the above spectral changes in the SC support the retardation action observed in our study of N-0915–ethanol.

Similar to the N-0915–ethanol and N-0915–PG formulations, spectral analysis of SC in presence of N-0915–PEG 400 showed an intense peak at 1760 and 1787 cm^{-1} representing a possible increase in lipid content (35). On the other hand, a blue shift was observed at 1637 cm^{-1} after N-0915–PEG 400 suggesting the weakening of the hydrogen bonds between the amide linkages of the ceramides. No other change in peak intensity or band shift was observed. Despite of the weakening of H-bonds at amide 1 linkage, it seems the appearance of two peaks near the 1735 cm^{-1} band (51) after N-0915–PEG 400 treatment were due to the retardation effect on SC.

DMBIS Formulations. The spectral analysis of DMBIS–water formulation (Fig. 4b) showed blue shifts at 3270 and 2917 cm^{-1} indicating lipid bilayer fluidization, increased SC hydration and lipid extraction by DMBIS treatment. Splitting of peaks around 1637 cm^{-1} was observed indicating change in protein conformation (formation of beta pleated sheets) that suggested permeation enhancement. At the same time, the blue shift at 1538 cm^{-1} suggested formation of strong H-bonds at the amide 2 band. The mechanism of action of DMBIS is similar to that of dimethyl sulfoxide (DMSO) (54). DMBIS initially binds to the free water from the formulation and if there is not sufficient free water present in the surroundings, it is thought to remove the protein-bound water molecules. As a result, structural changes occur in the SC proteins (evident by band splitting at amide 1 linkage and blue shift at amide 2 band) in order to improve intermolecular hydrogen bonding to compensate for the water loss. Like DMSO, the removal of protein-bound water is the reason for enhancement of the permeant in the presence of DMBIS–water formulation (55).

The infra-red spectrum of DMBIS–PG-treated SC showed a red shift around 3,270 and 1538 cm^{-1}. The red shift at 3270 cm^{-1} is because of removal of water by DMBIS (as described earlier) and shift at 1538 cm^{-1} is indicative of weakening of hydrogen bonds at the amide linkage. Also, the red shifts at the above band positions were accompanied by decrease in peak height, suggesting protein and lipid extraction. On the other hand, a significant blue shift occurred at 1637 cm^{-1} that indicated the enhancement action via weakening of H-bonds among the protein/ceramide molecules. The shifts at 1538 and 1637 cm^{-1} may also be due to the interaction of DMBIS–PG with skin proteins (36,54). Since the DMBIS–PG formulation contained no water, DMBIS removed SC protein-bound water leading to significant structural changes in the protein structure and therefore led to enhancement of the permeant. No other change in peak shifts or intensity was observed. All the above data suggest enhancement in presence of DMBIS–PG. Our results corroborate results of mechanistic testing performed by Song using confocal Raman microscopy technique, where significant interactions of DMBIS–PG formulation were observed at amide 1 linkage (54).

The FTIR analysis of SC after DMBIS–ethanol formulation application showed a red band shift at 3270 cm^{-1}. At the same band positions, a decrease in intensities of the signals was observed suggesting lipid extraction. At the same time, significant band splitting was observed at positions 1637 and 1538 cm^{-1} with significant decrease in corresponding signal intensities that suggests enhancement via protein or

lipid interactions, or both. The mechanism of enhancement of permeant followed by application of DMBIS–ethanol formulation (like other DMBIS-containing formulations) was due to removal of SC protein-bound water (55), which increased in the presence of ethanol in the formulation (evident by significant band splitting at amide 1 and amide linkages). Other bands did not indicate any shift or change in signal intensity.

The DMBIS–PEG 400 formulation when applied to SC showed red shift at 3270 cm^{-1} (observed in most DMBIS formulation due to removal of water from SC) with reduced peak intensity at the signal. At the same time, the DMBIS–PEG 400 formulation showed blue shifts at 1735 and 1637 cm^{-1} accompanied by decrease in peak intensity. In addition, splitting of amide 2 linkage was observed. All these observations suggest enhancement in presence of DMBIS–PEG 400 (also seen in *in vitro* permeation of DEET) by structural change in protein structure due to loss of water from SC protein (56).

DMMCBI Formulations. Unlike DMBIS, DMMCBI do not possess similarity to DMSO in modification of SC. The FTIR analysis of SC following DMMCBI–water application (Fig. 5b) showed a blue shift at band positions of 3270 and 1637 cm^{-1} and a red shift at 1735 cm^{-1} position. The *in vitro* permeation of DEET after application of DMMCBI–water showed enhancement as compared to no treatment but retardation as compared to water alone treatment. It suggests that enhancement is due to presence of water in DMMCBI–water formulation (as evidenced by the blue shift) that leads to formation of an aqueous pathway (23) which indirectly leads to state of disorder in the SC lipid bilayer. The retardation was due to DMMCBI in the formulation (as evidenced by the red shift). The contrasting effect of DMMCBI and water in the formulation led to an insignificant effect on permeation of DEET in the *in vitro* experiments when comparison of DEET permeation in presence of DMMCBI–water treatment and water alone treatment were performed in our previous study (3).

In spectral analysis of SC after application of DMMCBI–PG, blue shifts (44) and decrease in peak intensities (35) at different bands explain the enhancement of permeant (DEET) in presence of DMMCBI–PG formulation.

The stratum corneum spectral analysis following treatment with DMMCBI–ethanol formulation showed red shifts at 1735, 1637, 1538, and 1455 cm^{-1} band positions. This observation (except red shift at 1538 cm^{-1}) implies the development of an ordered state within the SC (41). Also, intense peaks at 1724 and 1779 cm^{-1} were observed suggesting the formation of H-bonds in the triglycerides in the region. All these changes support the establishment of stable organization of lipids and proteins in the SC, which is further supported by retardation of DEET permeation, as observed in the DMMCBI–ethanol formulation (3). Moreover, a blue shift was observed at symmetric band indicating that retardation activity of DMMCBI–ethanol formulation does not occur through the symmetric methylene stretching of the SC lipids.

When SC treated with DMMCBI–PEG formulation was analyzed by FTIR, a blue shift was observed at 1637 cm^{-1} and a red shift at 1538 cm^{-1} (44). Even though the observed shifts suggest enhancement in presence of DMMCBI–PEG 400

formulation, *in vitro* permeation studies indicated retardation of DEET. The observed retardation of DEET seemed to be due to PEG 400 in the formulation that acted as a physical barrier preventing the permeation of permeant across the SC.

TBDOC Formulations. The spectral analysis of SC treated with TBDOC–water formulation (Fig. 6b) depicted blue shifts at 3270, 1637 and 1538 cm^{-1} band positions. Even though the blue shift in case of amide 2 linkage (1518 cm^{-1}) is indicative of strong hydrogen bonds in the ceramide molecules; it may be possible that these interactions occurred between the water molecules present in the formulation and ceramide molecules in the stratum corneum leading to fluidization of lipid bilayer of SC. These shifts were also accompanied by decrease in peak heights suggesting that TBDOC–water formulation caused disorder in the stratum corneum along with lipid extraction and interactions with proteins. TBDOC–water formulation might have also led to increased hydration of SC (evident by blue shifts at 3270 and 1637 cm^{-1}) that might have created aqueous pore pathways in the SC that facilitated the diffusion of permeant (23). This hypothesis is supported by the evidence that *in vitro* permeation enhancement of DEET was observed in presence TBDOC–water.

In spectral analysis of TBDOC–PG-treated SC, the observation of blue shifts at 3270, 2917, 2850 cm^{-1} suggest enhancement due to disorder in the lipid arrangement by the TBDOC–PG formulation by its impact on alkyl chain organization (32,44). The red shift at 1735 cm^{-1} and blue shift at 1544 cm^{-1} suggest formation of strong H-bonds (44) that may be due to the presence of TBDOC in the formulation (a potential retardant). There was splitting of band at 1637 cm^{-1} position to yield peaks at 1639, 1627, and 1691 cm^{-1} suggesting reorientation (hydrogen bond) of the ceramide head groups with propylene glycol in the formulation leading to loosening of the organization of lipid bilayer. The amide 1 splitting also suggests formation of distorted beta pleated structure of keratin that contributed to enhancement of the permeant in presence of TBDOC–PG.

In spectral analysis of SC treated with TBDOC–ethanol, blue shifts were observed at 2850 and 1544 cm^{-1} positions along with appearance of peak at 1710 cm^{-1} (red shift). The blue shift at 1544 cm^{-1} suggests the formation of strong hydrogen bonds among the ceramides (44). Furthermore, peak splitting at 1637 cm^{-1} band was also observed. However, there was no shift seen at the 3270 and 2917 cm^{-1}. The above observation suggests that TBDOC–ethanol formulation act as retardant by its action on amide 2 linkage and lipid ester linkage.

TBDOC–PEG 400 formulation-treated SC showed similar spectral bands like TBDOC–ethanol, except it showed blue shift at 3270 cm^{-1} (57) leading to its enhancement action due to increased hydration of SC (25).

The spectral and thermal analysis in this study showed distinct effects on structure and composition of SC that have played a role in affecting flux of DEET in our previous study (3). However, the residual penetration modifier formulation left on top of the SC influenced DEET permeation and its partitioning into the SC. All formulations were filtered prior to application on the donor skin samples (3).

CONCLUSION

In this study, DSC and IR techniques showed that each penetration modifier formulation caused unique changes in SC lipid organization that in turn led to modification of their inherent enhancer/retardant activity. We observed that penetration modifier formulations that enhanced the permeation of active acted mainly by disruption and fluidization of the lipid bilayer as evidenced by characteristic lowering of mean transition temperature and occurrence of blue shifts at characteristic frequencies with additional decline in peak intensity. On the other hand, thermal and spectral analyses of penetration modifier formulations showing retardation depicted elevated T_{m2}, certain red shifts and formation of multiple peaks around 1738 cm^{-1} transition suggesting retardation by strengthening of lipid–protein complex and organization of SC lipids by increased H-bonding. However, thermal and spectral analyses did not reveal the reason for the intensity of enhancement/retardation in presence of each formulation. Though additional analytical techniques such as confocal microscopy, X-ray diffractometry, and freeze fracture microscopy would have conclusively explained mechanism of penetration modifier formulations, our study utilized DSC and FTIR as the analytical techniques to shed at least partial light on the mechanism of action of penetration modifier formulations. The results from this study provided preliminary explanation for the effects of penetration modifier formulations. *In vivo* studies are being planned to further explain the mechanism of action of the penetration modifier formulations since more investigation is warranted to provide insights for the degree of enhancement or retardation in these complex systems.

ACKNOWLEDGMENTS

REFERENCES

1. Wertz PW. Epidermal lipids. Semin Dermatol. 1992;11(2):106–13.
2. Kaushik D, Batheja P, Kilfoyle B, Rai V, Michniak-Kohn B. Percutaneous permeation modifiers: enhancement *versus* retardation. Expert Opin Drug Deliv. 2008;5(5):517–29.
3. Kaushik D, Costache A, Michniak-Kohn B. Percutaneous penetration modifiers and formulation effects. Int J Pharm. 2010;386(1–2):42–51.
4. Hoogstraate AJ, Verhoef J, Brussee J, IJzerman AP, Spies F, Boddé HE. Kinetics, ultrastructural aspects and molecular modelling of transdermal peptide flux enhancement by N-alkylazacycloheptanones. Int J Pharm. 1991;76(1–2):37–47.
5. Sintov AC, Zhang PJ, Michniak-Kohn BB. Cutaneous biotransformation of N-(4-bromobenzoyl)-S,S-dimethyliminosulfurane and its product, 4-bromobenzamide, leading to percutaneous penetration enhancement of drugs: initial evidence using hydrocortisone. J Control Release. 2009;133(1):44–51.
6. Hadgraft J, Peck J, Williams DG, Pugh WJ, Allan G. Mechanisms of action of skin penetration enhancers/retarders: Azone and analogues. Int J Pharm. 1996;141(1–2):17–25.
7. Kim N, El-Khalili M, Henary MM, Strekowski L, Michniak BB. Percutaneous penetration enhancement activity of aromatic S,S-dimethyliminosulfuranes. Int J Pharm. 1999;187(2):219–29.
8. Purdon C. Synthesis and evaluation of aminocaprolactam derivatives as novel skin penetration retarders. [Ph.D. Thesis]. College of Pharmacy, University of South Carolina, Columbia; 2005.
9. Williams A, Barry, BW. Chemical Permeation enhancement. In: Touitou E, Barry, BW, editor. Enhancement in drug delivery. CRC, Taylor & Francis Group; 2006. p. 233–254.
10. Kasting GB, Bhatt VD, Speaker TJ. Microencapsulation decreases the skin absorption of N,N-diethyl-m-toluamide (DEET). Toxicol *In Vitro*. 2008;22(2):548–52.
11. Iscan Y, Hekimoglu S, Sargon MF, Hincal AA. DEET-loaded solid lipid particles for skin delivery: *in vitro* release and skin permeation characteristics in different vehicles. J Microencapsul. 2006;23(3):315–27.
12. Golden GM, Guzek DB, Kennedy AH, McKie JE, Potts RO. Stratum corneum lipid phase transitions and water barrier properties. Biochemistry. 1987;26(8):2382–8.
13. Sapra B, Jain S, Tiwary AK. Percutaneous permeation enhancement by terpenes: mechanistic view. AAPS J. 2008;10(1):120–32.
14. Windheuser JJ, Haslam JL, Caldwell L, Shaffer RD. The use of N,N-diethyl-m-toluamide to enhance dermal and transdermal delivery of drugs. J Pharm Sci. 1982;71(11):1211–3.
15. Van Duzee BF. Thermal analysis of human stratum corneum. J Invest Dermatol. 1975;65(4):404–8.
16. Golden GM, Guzek DB, Harris RR, McKie JE, Potts RO. Lipid thermotropic transitions in human stratum corneum. J Invest Dermatol. 1986;86(3):255–9.
17. Potts R, Golden GM, Francoeur ML, Mak VHW, Guy RH. Mechanism and enhancement of solute transport across the stratum corneum. J Control Release. 1991;15:249–60.
18. Leopold CS, Lippold BC. An attempt to clarify the mechanism of the penetration enhancing effects of lipophilic vehicles with differential scanning calorimetry (DSC). J Pharm Pharmacol. 1995;47(4):276–81.
19. Tanojo H, Bouwstra JA, Junginger HE, Bodde' HE. Thermal analysis studies on human skin and skin barrier modulation by fatty acids and propylene glycol. J Therm Anal Calorim. 1999;57(1):313–22.
20. Yamane MA, Williams AC, Barry BW. Effects of terpenes and oleic acid as skin penetration enhancers towards 5-fluorouracil as assessed with time; permeation, partitioning and differential scanning calorimetry. Int J Pharm. 1995;116(2):237–51.
21. Cornwell PA, Barry BW, Stoddart CP, Bouwstra JA. Wide-angle X-ray diffraction of human stratum corneum: effects of hydration and terpene enhancer treatment. J Pharm Pharmacol. 1994;46(12):938–50.
22. Van Hal DA, Jeremiasse E, Junginger HE, Spies F, Bouwstra JA. Structure of fully hydrated human stratum corneum: a freeze-fracture electron microscopy study. J Invest Dermatol. 1996;106(1):89–95.
23. Menon GK, Elias PM. Morphologic basis for a pore-pathway in mammalian stratum corneum. Skin Pharmacol. 1997;10(5–6):235–46.
24. Ogiso T, Iwaki M, Bechako K, Tsutsumi Y. Enhancement of percutaneous absorption by laurocapram. J Pharm Sci. 1992;81(8):762–7.
25. Williams AC, Barry BW. Penetration enhancers. Adv Drug Deliv Rev. 2004;56(5):603–18.
26. Francoeur ML, Golden GM, Potts RO. Oleic acid: its effects on stratum corneum in relation to (trans)dermal drug delivery. Pharm Res. 1990;7(6):621–7.
27. Melot M, Pudney PD, Williamson AM, Caspers PJ, Van Der Pol A, Puppels GJ. Studying the effectiveness of penetration enhancers to deliver retinol through the stratum cornum by *in vivo* confocal Raman spectroscopy. J Control Release. 2009;138(1):32–9.
28. Lawson E, Edwards HGM, Williams AC, Barry BW. Applications of Raman spectroscopy to skin research. Skin Res Technol. 1997;3(3):147–53.
29. Cornwell PA, Barry BW, Bouwstra JA, Gooris GS. Modes of action of terpene penetration enhancers in human skin; Differential

scanning calorimetry, small-angle X-ray diffraction and enhancer uptake studies. Int J Pharm. 1996;127(1):9–26.

30. Mantsch HH, Chapman D. Infrared spectroscopy of biomolecules. New York: Wiley-Liss; 1996.

31. Garidel P. Mid-FTIR- Microspectroscopy of stratum corneum single cells and stratum corneum tissue. Phys Chem Chem Phys. 2002;4:5671–7.

32. Panchagnula R, Salve PS, Thomas NS, Jain AK, Ramarao P. Transdermal delivery of naloxone: effect of water, propylene glycol, ethanol and their binary combinations on permeation through rat skin. Int J Pharm. 2001;219(1–2):95–105.

33. Tamm LK, Tatulian SA. Infrared spectroscopy of proteins and peptides in lipid bilayers. Q Rev Biophys. 1997;30(4):365–429.

34. Garidel P, Blume A, Hubner W. A Fourier transform infrared spectroscopic study of the interaction of alkaline earth cations with the negatively charged phospholipid 1, 2-dimyristoyl-*sn*-glycero-3-phosphoglycerol. Biochim Biophys Acta. 2000;1466(1–2):245–59.

35. Mendelsohn R, Chen HC, Rerek ME, Moore DJ. Infrared microspectroscopic imaging maps the spatial distribution of exogenous molecules in skin. J Biomed Opt. 2003;8(2):185–90.

36. Zhang G, Moore DJ, Flach CR, Mendelsohn R. Vibrational microscopy and imaging of skin: from single cells to intact tissue. Anal Bioanal Chem. 2007;387(5):1591–9.

37. Zhang G, Moore DJ, Mendelsohn R, Flach CR. Vibrational microspectroscopy and imaging of molecular composition and structure during human corneocyte maturation. J Invest Dermatol. 2006;126(5):1088–94.

38. Brandenburg K, Seydel U. Infrared spectroscopy of glycolipids. Chem Phys Lipids. 1998;96(1–2):23–40.

39. Nair VB, Panchagnula R. Effect of iontophoresis and fatty acids on permeation of arginine vasopressin through rat skin. Pharmacol Res. 2003;47(6):563–9.

40. Takahashi K, Sakano H, Numata N, Kuroda S, Mizuno N. Effect of fatty acid diesters on permeation of anti-inflammatory drugs through rat skin. Drug Dev Ind Pharm. 2002;28(10):1285–94. doi:10.1081/DDC-120015362.

41. Dias M, Naik A, Guy RH, Hadgraft J, Lane ME. *In vivo* infrared spectroscopy studies of alkanol effects on human skin. Eur J Pharm Biopharm. 2008;69(3):1171–5.

42. Kim YC, Park JH, Ludovice PJ, Prausnitz MR. Synergistic enhancement of skin permeability by *N*-lauroylsarcosine and ethanol. Int J Pharm. 2008;352(1–2):129–38.

43. Mendelsohn R, Rerek ME, Moore DJ. Infrared spectroscopy and microscopic imaging of stratum corneum models and skin. Phys Chem Chem Phys. 2000;2(20):4651–7.

44. Garidel P. Calorimetric and spectroscopic investigations of phytosphingosine ceramide membrane organisation. Phys Chem Chem Phys. 2002;4:1934–42.

45. Moore DJ, Rerek ME. Insights into the molecular organization of lipids in the skin barrier from infrared spectroscopy studies of stratum corneum lipid models. Acta Derm Venereol Suppl (Stockh). 2000;208:16–22.

46. Lin SY, Duan KJ, Lin TC. Microscopic FT-IR/DSC system used to simultaneously investigate the conversion process of protein structure in porcine stratum corneum after pretreatment with skin penetration enhancers. Meth Find Exp Clin Pharmacol. 1996;18(3):175–81.

47. Bommannan D, Potts RO, Guy RH. Examination of the effect of ethanol on human stratum corneum *in vivo* using infrared spectroscopy. J Control Release. 1991;16(3):299–304.

48. Krill SL, Knutson K, Higuchi WI. Ethanol effects on the stratum corneum lipid phase behavior. Biochim Biophys Acta. 1992;1112 (2):273–80.

49. Krishnaiah YS, Satyanarayana V, Karthikeyan RS. Effect of the solvent system on the *in vitro* permeability of nicardipine hydrochloride through excised rat epidermis. J Pharm Pharm Sci. 2002;5(2):123–30.

50. Wotton PK, Møllgaard B, Hadgraft J, Hoelgaard A. Vehicle effect on topical drug delivery. III. Effect of azone on the cutaneous permeation of metronidazole and propylene glycol. Int J Pharm. 1985;24(1):19–26.

51. Amin S, Kohli K, Khar RK, Mir SR, Pillai KK. Mechanism of *in vitro* percutaneous absorption enhancement of carvedilol by penetration enhancers. Pharm Dev Technol. 2008;13 (6):533–9.

52. Berner B, Mazzenga GC, Otte JH, Steffens RJ, Juang RH, Ebert CD. Ethanol: water mutually enhanced transdermal therapeutic system II: skin permeation of ethanol and nitroglycerin. J Pharm Sci. 1989;78(5):402–7.

53. Levang AK, Zhao K, Singh J. Effect of ethanol/propylene glycol on the *in vitro* percutaneous absorption of aspirin, biophysical changes and macroscopic barrier properties of the skin. Int J Pharm. 1999;181(2):255–63.

54. Song Y, Xiao C, Mendelsohn R, Zheng T, Strekowski L, Michniak B. Investigation of iminosulfuranes as novel transdermal penetration enhancers: enhancement activity and cytotoxicity. Pharm Res. 2005;22(11):1918–25.

55. Greve T, Andersen K, Nielsen O. Penetration mechanism of dimethyl sulfoxide in human and pig ear skin: an ATR–FTIR and near-FT Raman spectroscopic *in vivo* and *in vitro* study. Spectrosc Int J. 2008;22(5):405–17.

56. Barry BW. Mode of action of penetration enhancers in human skin. J Control Release. 1987;6(1):85–97.

57. Schneider A, Middaugh CR, Oldewurtel MD. Role of bound water in biological membrane structure: fluorescence and infrared studies. J Supramol Struct. 1979;10(2):265–75.